AD-A241 801

Reconstruction at Ordered Au(110)-Aqueous Interfaces as Probed

by Atomic-Resolution Scanning Tunneling Microscopy

by

X. Gao, A. Hamelin, and M.J. Weaver

Prepared for Publication

in the

Physical Review B.

DTIC
ELECTE
OCT 16 1991
S D
D

Purdue University

Department of Chemistry

West Lafayette, Indiana 47907

October 1991

91-13308

REPORT DOCUMENTATION PAGE

Form Approved
OMB No 0704 0188

1a. REPORT SECURITY CLASSIFICATION Unclassified	1b. RESTRICTIVE MARKINGS
2a. SECURITY CLASSIFICATION AUTHORITY	3. DISTRIBUTION/AVAILABILITY OF REPORT Approved for public release and sale; its
2b DECLASSIFICATION/DOWNGRADING SCHEDULE	distribution is unlimited.

4. PERFORMING ORGANIZATION REPORT NUMBER(S) Technical Report No. 110	5. MONITORING ORGANIZATION REPORT NUMBER(S)

6a. NAME OF PERFORMING ORGANIZATION Purdue University Department of Chemistry	6b. OFFICE SYMBOL (If applicable)	7a. NAME OF MONITORING ORGANIZATION Division of Sponsored Programs Purdue Research Foundation
6c ADDRESS (City, State, and ZIP Code) Purdue University Department of Chemistry West Lafayette, IN 47907-1393		7b. ADDRESS (City, State, and ZIP Code) Purdue University West Lafayette, IN 47907

8a. NAME OF FUNDING/SPONSORING ORGANIZATION Office of Naval Research	8b. OFFICE SYMBOL (If applicable)	9 PROCUREMENT INSTRUMENT IDENTIFICATION NUMBER Contract No. N00014-91-J-1409

8c. ADDRESS (City, State, and ZIP Code) 800 N. Quincy Street Arlington, VA 22217	10. SOURCE OF FUNDING NUMBERS			
	PROGRAM ELEMENT NO.	PROJECT NO.	TASK NO	WORK UNIT ACCESSION NO

11. TITLE (Include Security Classification)
Reconstruction at Ordered Au(110)-Aqueous Interfaces as Probed by Atomic-Resolution Scanning Tunneling Microscopy

12. PERSONAL AUTHOR(S)
X. Gao, A. Hamelin, and M.J. Weaver

13a. TYPE OF REPORT Technical	13b. TIME COVERED FROM _____ TO _____	14. DATE OF REPORT (Year, Month, Day) October 31, 1991	15. PAGE COUNT

16. SUPPLEMENTARY NOTATION

17. COSATI CODES			18. SUBJECT TERMS (Continue on reverse if necessary and identify by block number)
FIELD	GROUP	SUB-GROUP	Atomic-resolution scanning tunneling microscopy images of ordered Au(110), surface reconstruction, three-atom wide ribbons

19. ABSTRACT (Continue on reverse if necessary and identify by block number)

Atomic-resolution scanning tunneling microscopy (STM) images of ordered Au(110) in aqueous 0.1 $\underline{M}$ HClO$_4$, reported as a function of electrode potential, provide an unusually detailed picture of surface reconstruction. Lowering the potential of a freshly annealed surface to -0.3 V vs SCE yield images consisting primarily of domains having (1 x 2) symmetry. While the (1 x 2) structure exhibits an atomic density commensurate with the usual "missing-row" model, the images suggest that significant relaxation of both top- and second-layer atoms occurs. Three-atom wide ribbons, lying along the [1$\bar{1}$0] direction, are seen to provide the basic building blocks of the reconstruction; these units also yield "added-row" domains of (1 x n) symmetry, where n = 3 or higher. The reconstruction is lifted, yielding the (1 x 1) Au(110) surface, rapidly (within ca 2s) upon altering the potential to 0 V vs SCE, yet reappears immediately upon returning to -0.3 V.

20. DISTRIBUTION/AVAILABILITY OF ABSTRACT ☐ UNCLASSIFIED/UNLIMITED ☐ SAME AS RPT. ☐ DTIC USERS	21. ABSTRACT SECURITY CLASSIFICATION
22a NAME OF RESPONSIBLE INDIVIDUAL	22b TELEPHONE (Include Area Code)	22c OFFICE SYMBOL

DD Form 1473, JUN 86   Previous editions are obsolete.   SECURITY CLASSIFICATION OF THIS PAGE

ABSTRACT

Atomic-resolution scanning tunneling microscopy (STM) images of ordered Au(110) in aqueous 0.1 $\underline{M}$ HClO$_4$, reported as a function of electrode potential, provide an unusually detailed picture of surface reconstruction. Lowering the potential of a freshly annealed surface to −0.3 V vs SCE yield images consisting primarily of domains having (1 x 2) symmetry. While the (1 x 2) structure exhibits an atomic density commensurate with the usual "missing-row" model, the images suggest that significant relaxation of both top- and second-layer atoms occurs. Three-atom wide ribbons, lying along the [1$\bar{1}$0] direction, are seen to provide the basic building blocks of the reconstruction; these units also yield "added-row" domains of (1 x n) symmetry, where n = 3 or higher. The reconstruction is lifted, yielding the (1 x 1) Au(110) surface, rapidly (within ca 2s) upon altering the potential to 0 V vs SCE, yet reappears immedia'ely upon returning to −0.3 V.

As for metal surfaces in ultrahigh vacuum (uhv), elucidating the occurrence and nature of reconstruction at ordered electrochemical interfaces is a topic of major fundamental and practical importance. While reconstruction has long been considered to occur at metal-solution interfaces, especially for gold low-index faces on the basis of conventional electrochemical measurements,[1] detailed information has been lacking due to the paucity of suitable "in-situ" structural probes. Both second harmonic generation (SHG)[2] and x-ray diffraction[3] have recently proved useful as in-situ probes at ordered gold electrodes. However, the former yields little structural information, and the latter approach is limited in part by the availability of synchrotron x-ray sources.

A very promising technique for this purpose is scanning tunneling microscopy (STM) since it can yield local real-space structural information. While few STM studies of in-situ electrochemical systems have achieved the necessary atomic resolution, some recent reports demonstrate that such STM images can be observed under favorable circumstances at metal-solution interfaces.[4-8] One such study from our laboratory, involving Au(100) in aqueous 0.1 $\underline{M}$ HClO$_4$, illustrates that remarkably detailed information on potential-induced surface reconstruction can be obtained from in-situ STM.[8] Specifically, the (1 x 1) Au(100) surface is transformed into corrugated quasi-hexagonal domains having primarily a (5 x 27) symmetry by altering the potential below -0.25 V vs saturated calomel electrode (SCE); the reconstruction can be lifted by returning to 0.2 V.

Reported here is a preliminary account of related measurements performed for Au(110). The reconstruction of this surface in uhv has been examined extensively by low energy electron diffraction (LEED),[9-11] ion scattering,[12-14] x-ray diffraction,[15] electron microscopy,[16] and STM.[17] A predominantly (1 x 2) symmetry is observed, which is most commonly interpreted in terms of a "missing-

(or added-) row" structure (e.g., ref. 15b). Besides giving uniquely detailed information of such reconstruction on the Au(110) electrochemical surface, the present STM images provide some insight into the formation mechanism.

The Au(110) crystal (hemisphere, 5 mm diameter) was grown, cut, and polished in LEI-CNRS as outlined in ref. 18. The crystal was flame annealed immediately before each experiment, cooled in ultrapure water, and transferred to the STM cell protected by a drop of water. Details of the in-situ STM procedures are mostly as outlined in ref. 8 and 19. The microscope is a commercial Nanoscope II instrument (Digital Instruments, Inc.). The atomic-resolution STM images were obtained in the "constant current" mode. The set-point current, i_t, was typically 30 nA, and the bias voltage, V_b, was usually 4-10 mV. After assembling the STM cell with the freshly annealed crystal, aqueous 0.1 $\underline{M}$ $HClO_4$ was added, and a cyclic voltammogram (50 mV s^{-1}) usually recorded to check the surface state.

Unlike Au(100),[8] satisfactory atomic-resolution images were usually not obtained initially at potentials within the range -0.1 to 0.2 V vs SCE. However, altering the potential to -0.3 to -0.4 V yielded atomic-resolution images of consistently high quality. Figure 1 shows a typical *unfiltered* large-scale (180 x 180Å) image obtained at -0.3 V vs SCE. (The "height-shaded" view is 30° from the surface normal.) Stacked sets of parallel ribbon segments, located along the [1$\bar{1}$0] direction, are clearly seen. The spacing between these ribbons is mostly (4.0 x n)Å, where n - 2 or 3, i.e., corresponding to (1 x 2) and (1 x 3) symmetries. Figure 2 is a topview atomic-resolution image of a smaller (90 x 90Å) region. Each ribbon is clearly seen to consist of three parallel rows of gold atoms. The interatomic spacing along the [1$\bar{1}$0] direction is 2.9 ± 0.2Å, i.e., as for unreconstructed Au(110).

A closeup of a region containing mostly (1 x 2) reconstruction is shown in

Fig. 3. Information on the detailed surface atomic structure can be obtained from such STM images. While the overall symmetry and atomic density is consistent with the commonly proposed "missing-row" model, the present images indicate that some "surface relaxation" occurs, involving both the top and underlying atoms. In the conventional missing-row structure (depicted in Fig. 4A) the pairs of (unshaded) atoms either side of the central [1$\bar{1}$0] furrows are equivalent. The STM images, however, show that one of these rows in each unit cell is shifted by 1.45Å along the [1$\bar{1}$0] direction, the atoms of which appear less intense (i.e., are depressed in the Z-direction). Both these observations suggest that relaxation occurs so to form a slightly asymmetric structure as depicted in Fig. 4B. This ball model shows that such a top-layer relaxation should be accompanied by some pairing of the second-layer atoms, as can be seen in the side view of Fig. 4B. Also consistent with this "relaxed" structure are the corrugations obtained from the *constant-current* STM images, which indicate that the Z-displacements of the b,c atoms (see Fig. 4B) are 0.2 - 0.3Å and 0.4 - 0.6Å, respectively, below atom a. These observed Z-corrugations are markedly smaller than those anticipated for the unrelaxed missing-row structure (Fig. 4A).

A height-shaded STM image of a (1 x 3) surface region is shown in Fig. 5. (Note that the crystal has been rotated counterclockwise by ca 40° compared with the earlier figures.) Unlike the (1 x 2) structure, the rows of atoms on either side of the highest (i.e., brightest) rows are virtually unshifted along the [1$\bar{1}$0] direction. In this respect, then, the (1 x 3) structure seen here is similar to the usual "double missing-row" model.

Altering the potential in the positive direction resulted in an immediate (within 2s) disappearance of the reconstructed surface images by 0 V vs SCE, being replaced by images indicative of a (1 x 1) surface. Such an image is shown in Fig. 5. The (1 x 1) nature of the surface is evident from the spacing (4 ±

0.2Å) between the rows along the [001] direction. These potential-induced structural changes are largely reversible as well as rapid, the reconstruction reappearing within ca 2s when the potential is returned to -0.3 V.

Further inspection of the STM images provides some insight into the mechanism of reconstruction. The three-atom wide ribbons appear to provide basic "building blocks" from which the reconstruction is propagated. Examination of Fig. 1 shows that the longer-scale [i.e., (1 x 3), (1 x 4)] reconstructions occur by depositing such ribbons along the [1̄10] direction on the underlying terrace. In this sense, therefore, these structures can be viewed as "added-", rather than "missing-", row domains. The concerted motion of atoms required to form (or remove) such reconstructions appear to involve migration both across and along the rows. The small and rather irregular domain sizes observed here on Au(110) (e.g., Fig. 1) suggest that only short-range atomic motion is required.

The present results bear a similarity to in-situ STM data obtained on Au(100) in 0.1 M HClO$_4$, described elsewhere,[8] in that extensive reconstruction appears on both surfaces at ca -0.3 V and is lifted at 0 V and 0.2 V vs SCE for Au(110) and (100), respectively. An important difference, however, is that these structural transformations are much more rapid (as well as more reversible) on Au(110), requiring ca 10 mins on Au(100). The latter slow kinetics are consistent with the 24% additional gold atoms needed to form the reconstructed Au(100) surface,[8] presumably provided by long-range diffusional transport. The more rapid reconstruction dynamics on Au(110) are consistent with the requirement of only short-range motion of the ribbon segments.

It is worthy of note that the reconstruction on Au(110), as for Au(100), proceeds at potentials somewhat below the potential of zero charge [-0.02 V vs SCE for Au(110) in perchlorate media[20]], i.e., at small negative values of the surface electronic charge density, σ^m. While reconstruction of clean Au(110) in

uhv (i.e., at $\sigma^m = 0$) is spontaneous at room temperature, the formation of (1 x 3) as well as (1 x 2) structures is observed upon the deposition of alkali metals.[21] Since adsorption of such ionizable metals will yield negative σ^m values, some correspondence to the electrochemical case might be anticipated. Interestingly, adjusting σ^m to negative values is predicted to encourage reconstruction on (110) surfaces as a result of minimizing the kinetic energy of the sp electrons.[22]

The observation of (1 x 2) and (1 x 3) reconstruction on Au(110) at negative potentials in perchloric acid is in qualitative accord with LEED measurements following electrode emersion.[11] Inconsistent with the present results, however, is the report in ref. 11 that lifting the reconstruction on Au(110) requires large positive potentials, above 0.9 V vs SCE, where anodic oxide is formed. Given the facile nature of the Au(110) reconstruction process observed here, a rationalization of this discrepancy is that surface reconstruction on Au(110) is regenerated upon electrode emersion under the conditions in ref. 11 except in the presence of surface oxide. The results here may therefore signal a significant limitation of the use of electrode emersion, as opposed to strictly in-situ measurements (as for STM), as a means of probing surface reconstruction at electrochemical surfaces.

REFERENCES

1. A. Hamelin, J. Electroanal. Chem., 142, 299 (1982).

2. A. Friedrich, B. Pettinger, D.M. Kolb, G. Lüpke, R. Steinhoff, and G. Marowsky, Chem. Phys. Lett., 163, 123 (1989).

3. B.M. Ocko, J. Wang, A. Davenport, and H. Isaacs, Phys. Rev. Lett., 65, 1466 (1990).

4. O.M. Magnussen, J. Hotlos, R.J. Nichols, D.M. Kolb, and R.J. Behm, Phys. Rev. Lett., 64, 2929 (1990).

5. S.-C. Yau, C.M. Vitus, and B.C. Schardt, J. Am. Chem. Soc., 112, 3677 (1990).

6. S.-L. Yau, X. Gao, S.-C. Chang, B.C. Schardt, and M.J. Weaver, J. Am. Chem. Soc., 113, 6049 (1991).

7. C.M. Vitus, S.-C. Chang, B.C. Schardt, and M.J. Weaver, J. Phys. Chem., in press.

8. X. Gao, A. Hamelin, and M.J. Weaver, Phys. Rev. Lett., 67, 618 (1991).

9. (a) D. Wolf, H. Jagodzinski, and W. Moritz, Surface Sci., 77, 265 (1978); (b) W. Moritz and D. Wolf, Surface Sci., 163, L655 (1985).

10. J.R. Noonan and H.L. Davis, J. Vac. Sci. Tech., 16, 587 (1979).

11. (a) M.S. Zei, G. Lehmpful, and D.M. Kolb, Surface Sci., 221, 23 (1989); (b) R. Michaelis and D.M. Kolb, Surface Sci., 234, 6281 (1990).

12. S.H. Overbury, W. Heiland, D.M. Zehner, S. Datz, and R.S. Thoe, Surface Sci., 109, 239 (1981).

13. M. Copel and T. Gustafson, Phys. Rev. Lett., 57, 723 (1986).

14. J. Möller, H. Niehus, and W. Heiland, Surface Sci., 166, L111 (1986).

15. (a) I.K. Robinson, Phys. Rev. Lett., 50, 1145 (1983); (b) E. Vlieg, I.K. Robinson, and K. Kern, Surface Sci., 233, 248 (1990).

16. L.D. Marks, Phys. Rev. Lett., 51, 1000 (1983).

17. (a) G. Binnig, H. Rohrer, Ch. Gerber and E. Weibel, Surface Sci., 131, L379 (1983); (b) T. Gritsch, D. Coulman, R.J. Behm, and G. Ertl, Surface Sci., in press.

18. A. Hamelin, S. Morin, J. Richer, and J. Lipkowski, J. Electroanal. Chem., 285, 249 (1990).

19. S.-C. Chang, S.-L. Yau, B.C. Schardt, and M.J. Weaver, J. Phys. Chem., 95, 4787 (1991).

20. A. Hamelin and M.J. Weaver, J. Electroanal. Chem., 223, 171 (1987).

21. P. Häberle, P. Fenter, and T. Gustafsson, Phys. Rev. B., 39, 5810 (1989).

22. K-M. Ho and K.P. Bohnen, Phys. Rev. Lett., 59, 1833 (1987).

FIGURE CAPTIONS

Fig. 1

Unfiltered large-scale STM image, shown as height-shaded plot 30° from surface normal, of reconstruction on ordered Au(110) in 0.1 $\underline{M}$ HClO$_4$ at -0.3 V vs SCE

Fig. 2

Top view image showing (1 x 2) and (1 x 3) regions

Fig. 3

Height-shaded close-up image of largely (1 x 2) domain

Fig. 4

Ball-model (1 x 2) structures for: (A) conventional missing-row model, and (B) with relaxation as suggested by the STM images

Fig. 5

Height-shaded image of (1 x 3) domain

Fig. 6

Height-shaded image of (1 x 1) domain, formed by altering potential to 0 V vs SCE

[*Note to reviewers: the figures included with this ms. are Xerox copies of the original photographic prints, and are necessarily cf somewhat lower quality. The essential details of these images, as referred to in the text, however, are still largely discernable in these copies.*]
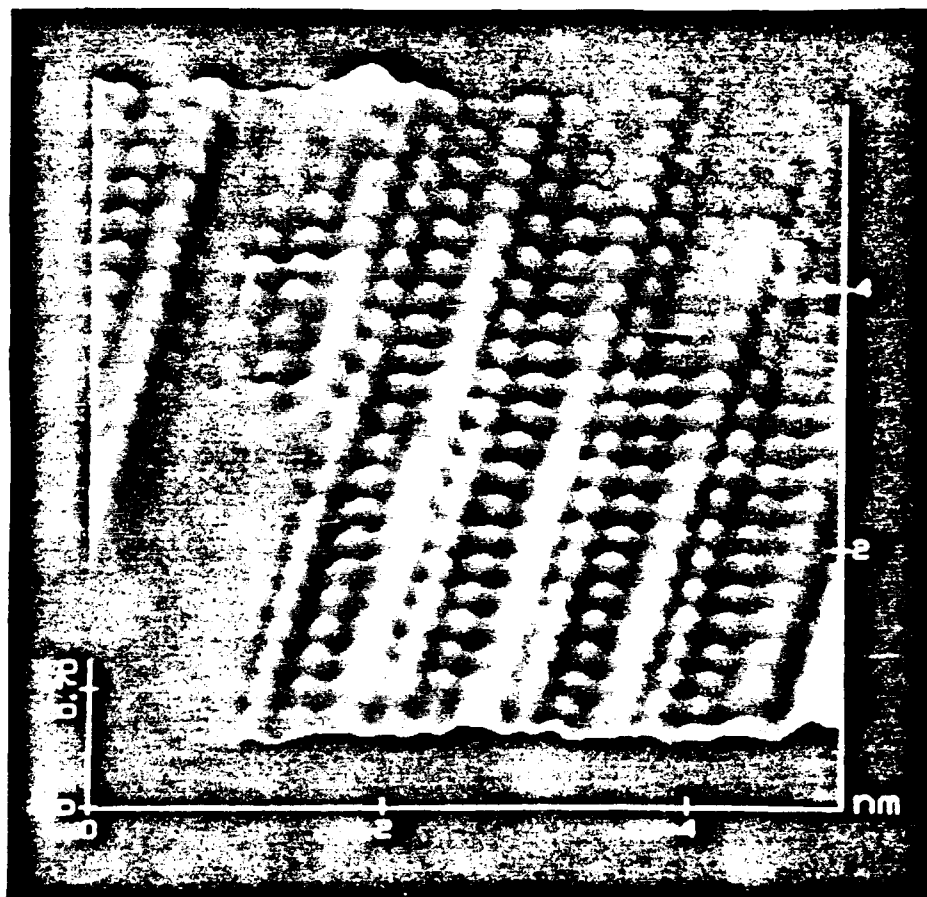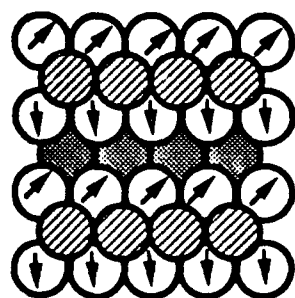
FIGURE 1
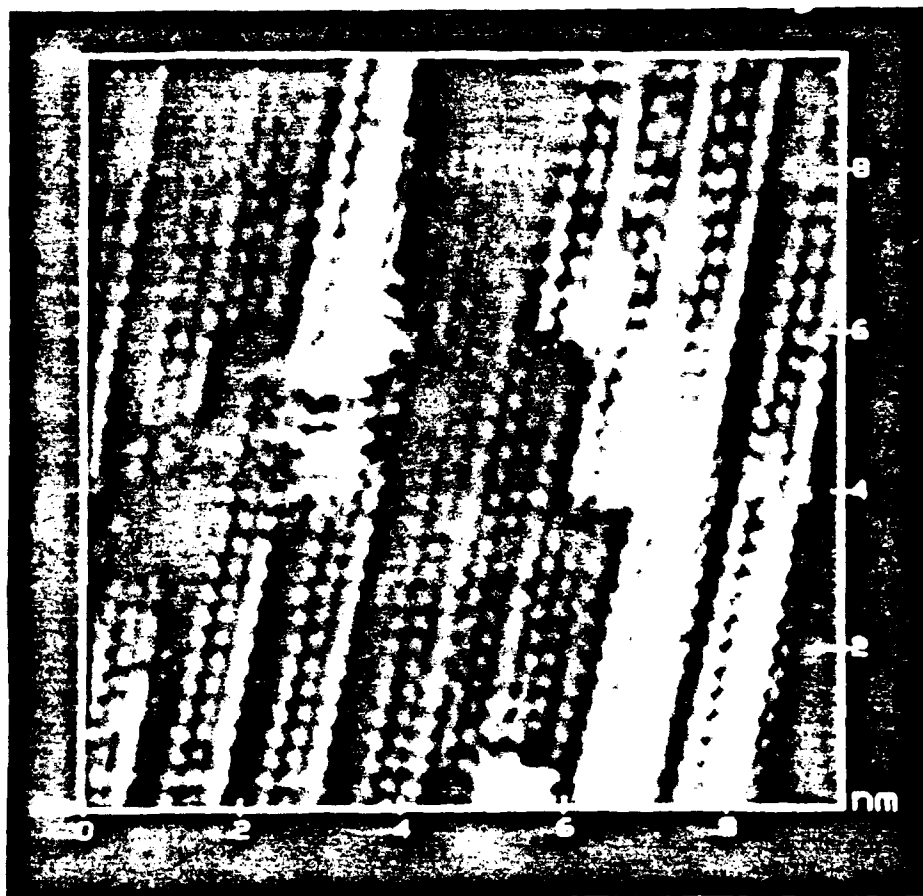
FIGURE 2

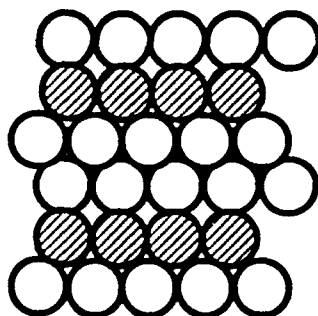FIGURE 3

Au(110) (1x2) structure

Top view   Side view

A   Missing row model

Relaxation
of missing
row model

a b c

B

Fig.4

FIGURE 5

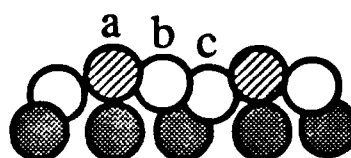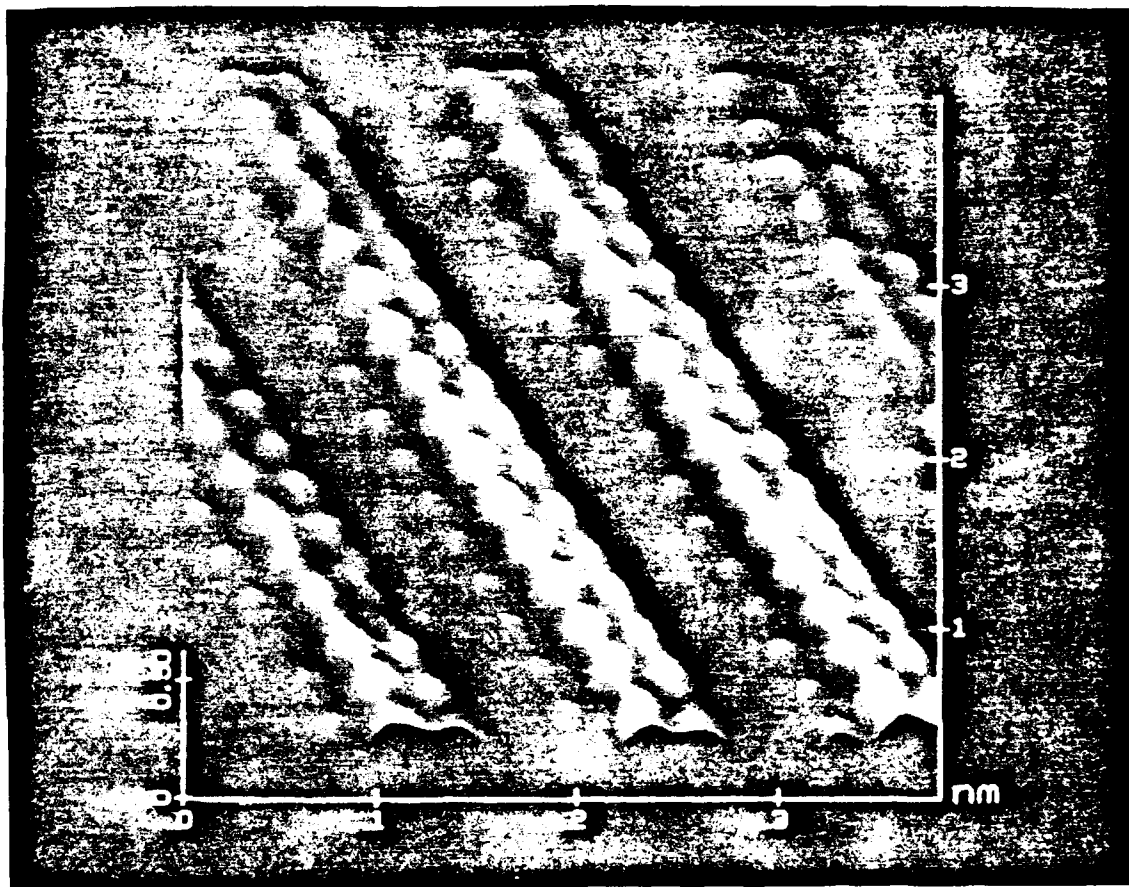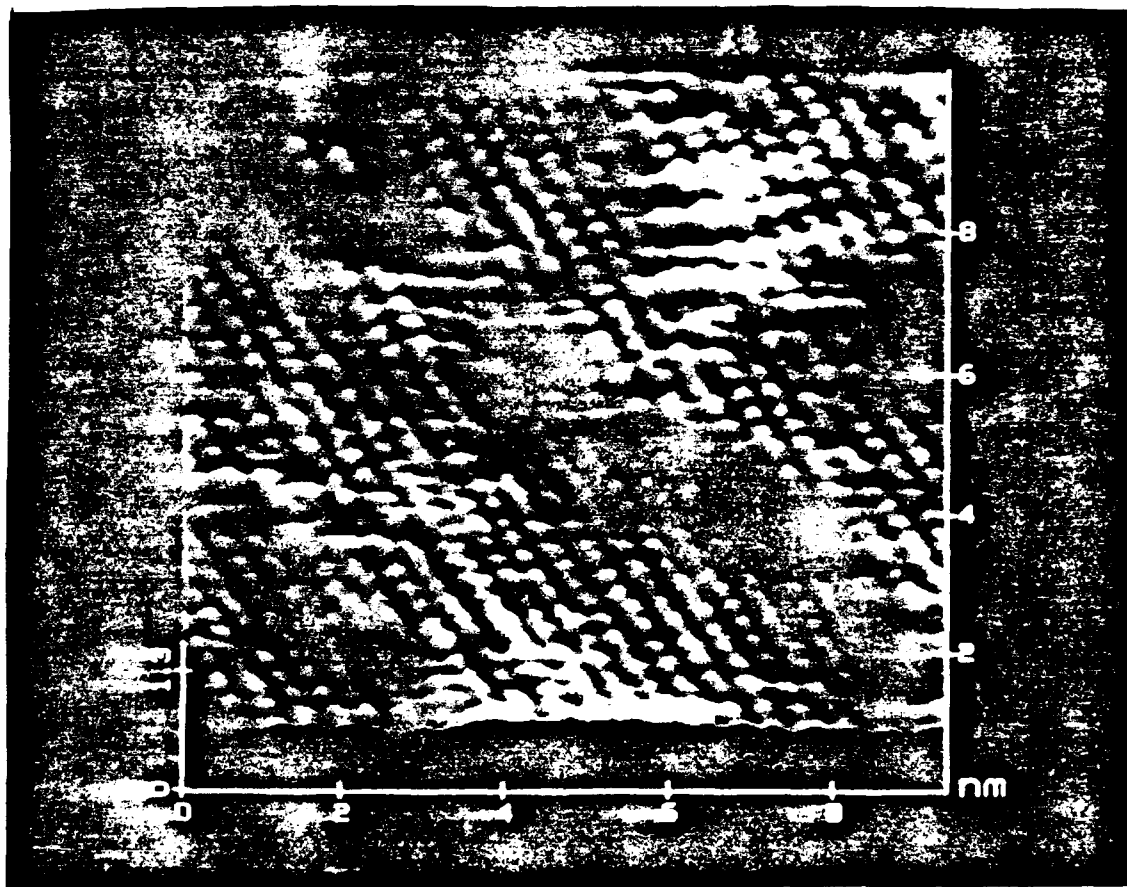FIGURE 6